Hindawi Publishing Corporation
Shock and Vibration
Volume 2016, Article ID 8902727, 13 pages
http://dx.doi.org/10.1155/2016/8902727

Research Article

Structural Performance Assessment Based on Statistical and Wavelet Analysis of Acceleration Measurements of a Building during an Earthquake

Mosbeh R. Kaloop,[1,2] Jong Wan Hu,[1,3] Mohamed A. Sayed,[4] and Jiyoung Seong[5]

[1]*Department of Civil and Environmental Engineering, Incheon National University, Incheon 406-840, Republic of Korea*
[2]*Department of Public Works and Civil Engineering, Mansoura University, Mansoura 35516, Egypt*
[3]*Incheon Disaster Prevention Research Center, Incheon National University, Incheon 406-840, Republic of Korea*
[4]*National Research Institute of Astronomy and Geophysics, Cairo 11421, Egypt*
[5]*National Disaster Management Institute, Ministry of Security and Public Administration, Seoul 121-719, Republic of Korea*

Correspondence should be addressed to Jong Wan Hu; jongp24@incheon.ac.kr

Received 3 September 2015; Accepted 21 October 2015

Academic Editor: Guillermo Rus

This study introduces the analysis of structural health monitoring (SHM) system based on acceleration measurements during an earthquake. The SHM system is applied to assess the performance investigation of the administration building in Seoul National University of Education, South Korea. The statistical and wavelet analysis methods are applied to investigate and assess the performance of the building during an earthquake shaking which took place on March 31, 2014. The results indicate that (1) the acceleration, displacement, and torsional responses of the roof recording point on the top floor of the building are more dominant in the X direction; (2) the rotation of the building has occurred at the base recording point; (3) 95% of the energy content of the building response is shown in the dominant frequency range (6.25–25 Hz); (4) the wavelet spectrum illustrates that the roof vibration is more obvious and dominant during the shaking; and (5) the wavelet spectrum reveals the elasticity responses of the structure during the earthquake shaking.

1. Introduction

Investigating the adequate and accurate performance of the structure at each stage of its life cycle is essential for elongating the life time of the structure. Based on analyses results, appropriate structural repairs and antiseismic retrofit methods can be planned. Moreover, applying various instrumental measurements in the structural health monitoring system is useful to decision makers [1].

Monitoring the performance of different types of structures is not widely employed in South Korea. Thus, the National Disaster Management Institute (NDMI) in South Korea targets to widely spread using the various structural performance tools in investigating and assessing the deformations of structures to mitigate the potential risk of conventional and inconvenient structures all around Korea. Furthermore, NDMI intends to obtain and develop a low cost monitoring system that will be able to improve the SHM of structures and to adequately increase the spread of the structural performance all around Korea. The improvement of monitoring tools aims also to develop data acquisition system and software that allow recording the structure responses to accurately and precisely obtain the structure deformations in near real-time [2].

The statistical analysis of the structural performance monitoring of structures is commonly used to test and asses the statistical modeling of buildings and statistical decision making for inferring the structure health state [3, 4]. Statistical time series methods for SHM are fundamentally of the inverse type [3, 5] and the structural decision making with specified performance characteristics. Kopsaftopoulos and Fassois [3] have introduced a study on the parametric

and nonparametric time series statistical methods which can be applied in SHM, where parametric times series statistical methods employ statistics based on parametric time series representation, while the nonparametric statistical methods employ statistics based on nonparametric representation [3, 5]. Fassois and Sakellariou [5] have summarized the time series statistical methods for the vibration of structures. Ding et al. [6] have applied the cross-correlation of SHM system to assess and predict the performance of bridge performance under different loads effects. Furthermore, they have found that the statistical analysis can detect the bridge abnormal performance under the varying environmental conditions. Kaloop et al. [7] and Kaloop and Hu [8] have applied a parametric model based on neural network to assess the performance of structures and for damage detection. They have found that the statistical analysis can be used in efficiently detecting the damage of structures.

Signal processing tools are used in amplitude and frequency analysis of the seismic waves velocities and of waves traveling paths within different soil layers with different properties [9]. The responses of structure under seismic loading are usually random and nonstationary. Therefore, they shall be preferably stochastically displayed using statistical time-varying techniques such as spectral density functions. The revolutionary wavelet analysis was shown to be a powerful signal processing tool [10].

Tibaduiza et al. [11] have illustrated and applied the principal component analysis and the wavelet analysis applications, related to statistical theory, in measuring the structural dynamic response signals and damage detection. Based on wavelet analysis, the statistical analysis of wavelet coefficients which are extracted from monitoring signals gave a representation that illustrates the energy distribution of the dynamic responses in time and frequency domains [11]. Dinh et al. [9] have demonstrated the seismic responses of a multispan structure based on wavelet analysis. They have found that the proposed wavelet analysis is a precise seismic tool for long span multisupport structures, since it accounts for the nonstationary in both amplitude and frequency of the excitations. In addition, it offers a realistic illustration of the energy content of the earthquake acceleration. Ali and Kim [12] have used wavelet analysis to analyze the seismic load effects of soil-structure-interaction on the base-isolated nuclear power plant. They have found that the wavelet analysis proves to be an efficient tool in investigating the effect of soil-structure-interaction on the frequency content of the acceleration response of base-isolated nuclear structure. Mollaioli and Bosi [13] have proposed the application of wavelet analysis on the seismic signals. They have found the construction of simplified signals containing the prominent features of the data distribution recorded from pulse-like earthquakes. Furthermore, many previous studies have applied the statistical and wavelet analysis in structural performance analysis and damage detection [14–17].

The proposed study aims to assess the structural performance of the administration building in Seoul National University of Education during an earthquake shaking. Moreover, investigating the structural performance is proposed based on a novel and simple application of nonparametric and parametric statistical methods and wavelet analysis. In addition, the assessment of the acceleration responses of the building is presented based on analyzing the wavelet energy content. Finally, checking the safety of the building and the low cost acceleration monitoring system efficiency are considered.

Table 1: Acceleration sensor performance.

Parameter	Description
Amplitude	4 g pk
Sensitivity	2.5 to 20 V/g
Dynamic range	165 dB
Bandwidth	DC to 200 Hz
Amplitude linearity	<0.1%

Table 2: Data-logger performance.

Parameter	Description
Sampling rate	1~1000 Hz
Synchronized accuracy	4 ms
Resolution	24 bit
Size	29.6 × 17.5 × 14.0 (mm)

2. Building and SHM Description

The case study structure is the 7-storey main administrative building at Seoul National University of Education. It is a reinforced concrete building that consists of seven storeys with total height of 26.5 as shown in Figure 1. The structural system of the building consists of reinforced concrete frames and core. The building has extensions in all directions as shown in Figure 1(c). The components of the SHM system are illustrated in Figure 2. The recorded data are digitized in a 24-bit analog-to-digital converter and then sent through a Bluetooth module and access point. All measured data are collected and then stored in a secure digital memory. One-channel acquisition devices are used in this study, whereas each acquisition device is synchronized by a signal sender from a computer at each time. The accelerometer properties are demonstrated in Table 1, while the data-logger performance is illustrated in Table 2. The acceleration sensors are used with maximum amplitude of 4 g. All devices are put inside boxes to protect them from different weather conditions such as rain, snow, or wind, as shown in Figure 3.

The arrangements of the acceleration measurement points are shown in Figures 1 and 4. Three monitoring points are located to monitor the responses of the building. The free-field (ground) point is located on the landscape, which surrounds the building to measure the free-field seismic shaking. The ground sensor point is 13.26 m from the building, as shown in Figure 4(a). Two measurement points are located on the building, which are the base point and the roof point. The base point is fixed in the building basement floor, while the roof point is fixed in the building roof as illustrated in Figure 4.

(a) Elevation view

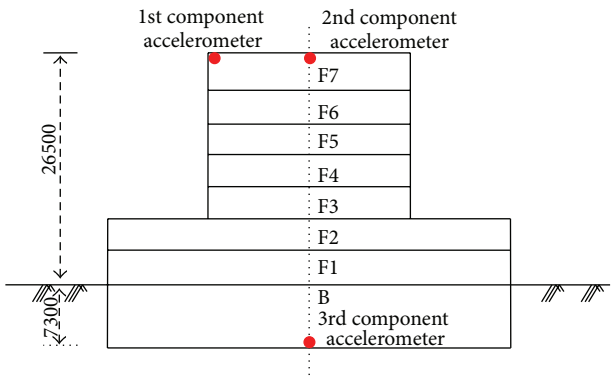

(b) Cross section

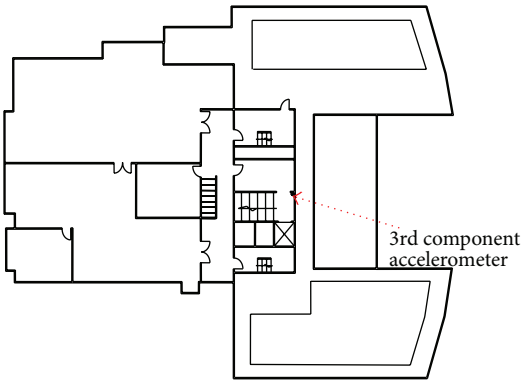

(c) Plan view

Figure 1: Administration building.

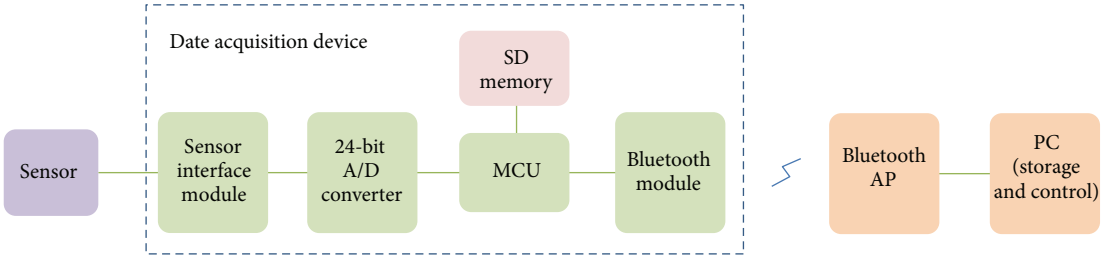

Figure 2: Structural monitoring system components.

(a) Acceleration sensor (b) Data-loggers and storage PC

Figure 3: Experimental setting of acceleration sensors at measuring points and SHM components.

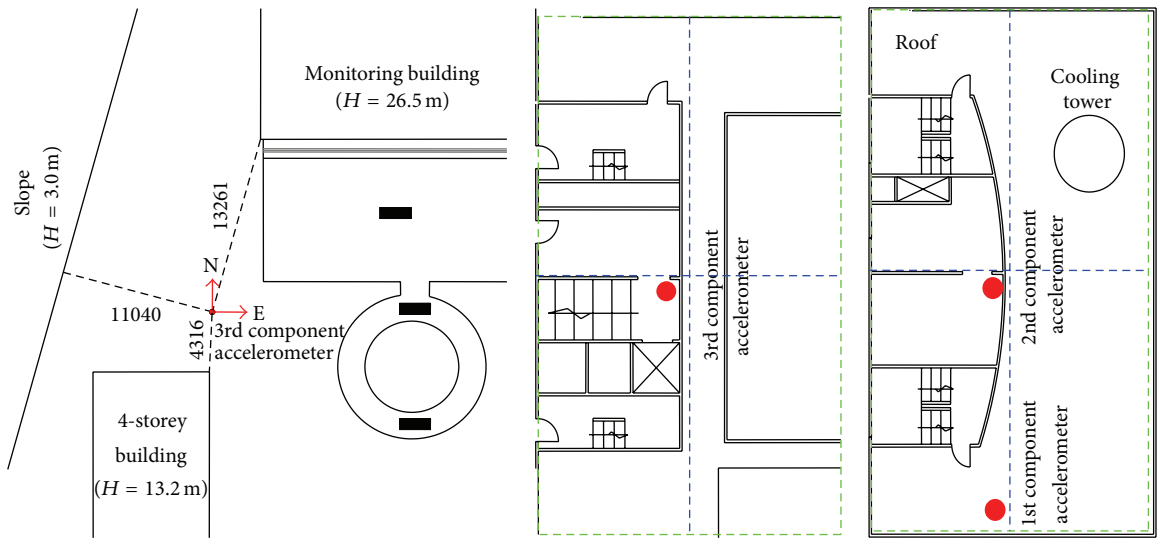

(a) Free-field (ground) point (b) Base point (c) Roof point

Figure 4: Monitoring points on the building.

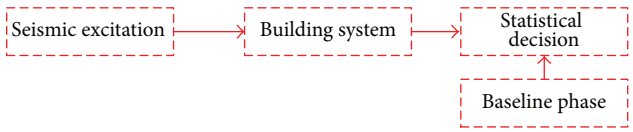

Figure 5: Scheme of the statistical decision of building.

3. Methodology and Results Analysis

3.1. Statistical Analysis. The statistical structural performance studies are summarized and presented in [3, 4, 16–18]. In civil engineering, structures properties may suffer slight deterioration with time or complete damage during severe events. Figure 5 is sketched based on the statistical structural performance conclusions drawn from Fassois and Sakellariou [5] and Arangio and Bontempi [18]. Statistical analysis provides boundary limits for the structural performance changes, and it is applied as warning for possible damages [16]. The majority of previous studies have used the parametric statistical analysis to assess the performance of structures [1–3, 7, 19, 20]. Therefore, the novel application of nonparametric (ellipse errors and covariance) and parametric (linear fitting) statistical analyses are utilized in this study to investigate the structural performance of the case study structure.

The acceleration measurements in Y direction at the ground point before and during the earthquake event are shown in Figure 6. The acceleration measurements are considered noises before the earthquake event, which implies no effective or peak values during the observations before the earthquake. However, the peak acceleration exceeded 3 Gal (cm/sec^2) during the earthquake as shown in Figure 6(b).

Figure 7 summarizes the peak acceleration of ground and roof points before and during the earthquake shaking. The maximum acceleration for the ground point was 0.64 Gal (cm/sec^2) and 3.42 Gal before and during the earthquake, respectively, in Y direction, while it was 0.50 Gal and 2.83 Gal before and during the earthquake, respectively, along X direction. In addition, the maximum acceleration of the base point was 0.03 Gal and 1.18 Gal before and during the earthquake, respectively, in the X direction, while it was 0.03 Gal and 0.70 Gal before and during the earthquake, respectively, in Y direction. Furthermore, the maximum acceleration at the roof point was 0.04 Gal and 4.84 Gal in X direction and 0.05 Gal and 2.50 Gal in Y direction, before and during the earthquake, respectively.

Figure 7 illustrates the linear fitting between the peak acceleration responses of base and roof points, with the ground point in X and Y directions. In addition, Figure 7 demonstrates that the roof response linear fitting (TX and TY) with ground response (GX and GY) is shown to be greater than that for the base response (BX and BY) for the two directions. Moreover, it can be seen that the X direction responses have the lowest peak values and the highest linear slope. From the results, it can be presented that the slopes are smaller than one in X and Y direction for the base point and in Y direction for the roof point. Furthermore, the slope is shown to be greater than one for the roof point in the X direction. It indicates that the effective direction of the structural responses occurred in X direction during the earthquake shaking.

Figure 8 depicts the ellipse errors with confidence 95% for the relation between the ground and building responses. It can be noticed from Figure 8 that the ellipse errors for the roof responses are higher than for the base responses. Moreover, it can be shown that the angles between the x-axis and the largest eigenvector for the building base and roof responses are 3.1416 rad and 3.1412 rad before the earthquake, while they are 3.1414 rad and 1.5706 rad during the earthquake, in X and Y direction, respectively. It indicates that

Table 3: Maximum eigenvalues and eigenvectors for covariance shaking point response matrix.

Parameters	Base point		Roof point	
	X	Y	X	Y
Eigenvalue	0.0072	0.0084	0.0229	0.0119
Eigenvector	$[-1; 1.45e-4]$	$[-1; 7.33e-5]$	$[1.55e-4; 1]$	$[7.24e-4; 1]$

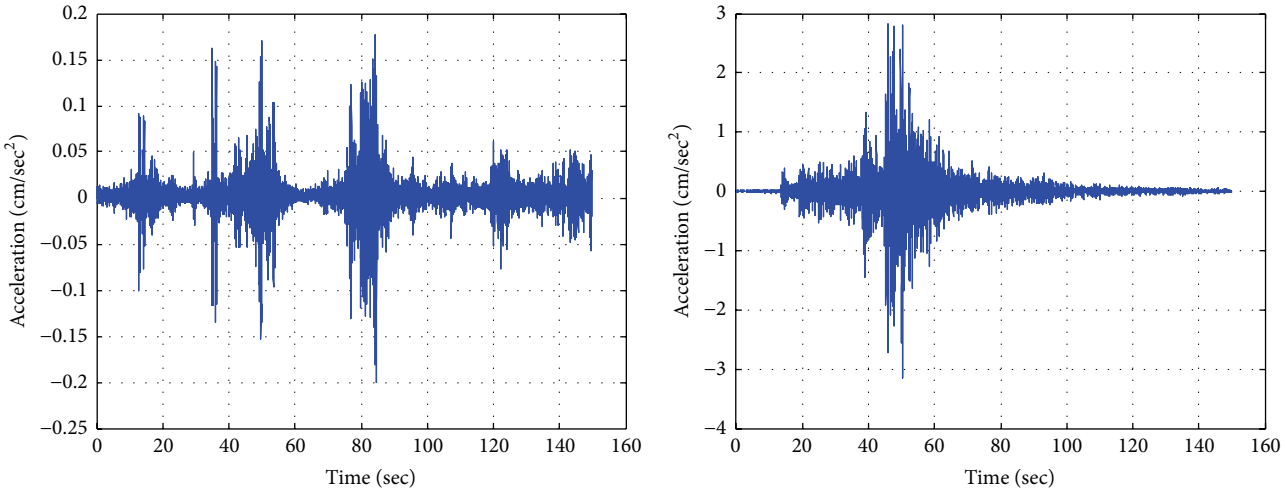

(a) Before the earthquake (b) During the earthquake

Figure 6: Acceleration response measurements at the ground point.

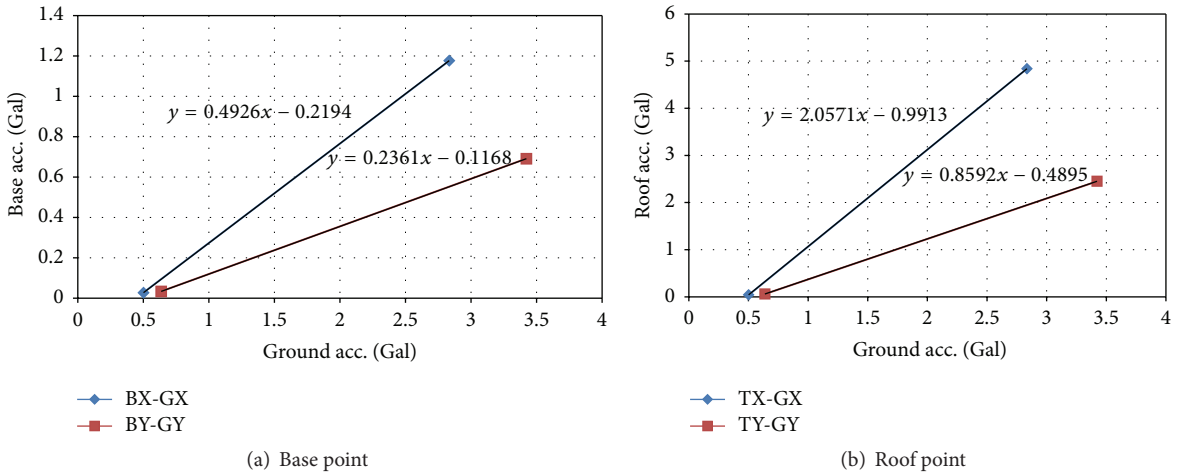

(a) Base point (b) Roof point

Figure 7: Linear fitting between the free-field response and the building different sensors responses.

the roof responses increased by 50% during the earthquake shaking for the two directions, while the base responses can be neglected during the shaking.

The covariance matrix of the base and roof acceleration responses is calculated with ground responses in X and Y directions. The results from the calculated covariance matrices show that the rotation occurred for the base point, while the hyperbolic rotation occurred for the roof point in the two directions. In addition, Table 3 illustrates the maximum eigenvalues and eigenvectors for the base and roof responses covariance matrices. From this table, it is shown that the roof eigenvalues and eigenvector are greater than for the base in the two directions, which assure the higher responses for the roof point under the earthquake shaking. From the previous statistical analysis, it is concluded that acceleration responses of the roof are higher and more effective in the X direction. In addition, the building rotation occurred at the base, while the hyperbolic rotation occurred at the roof. Finally, the previous statistical analysis results including ellipse errors, covariance, and linear fitting are sufficiently capable of investigating the performance of structures under earthquake loading, combined or separately.

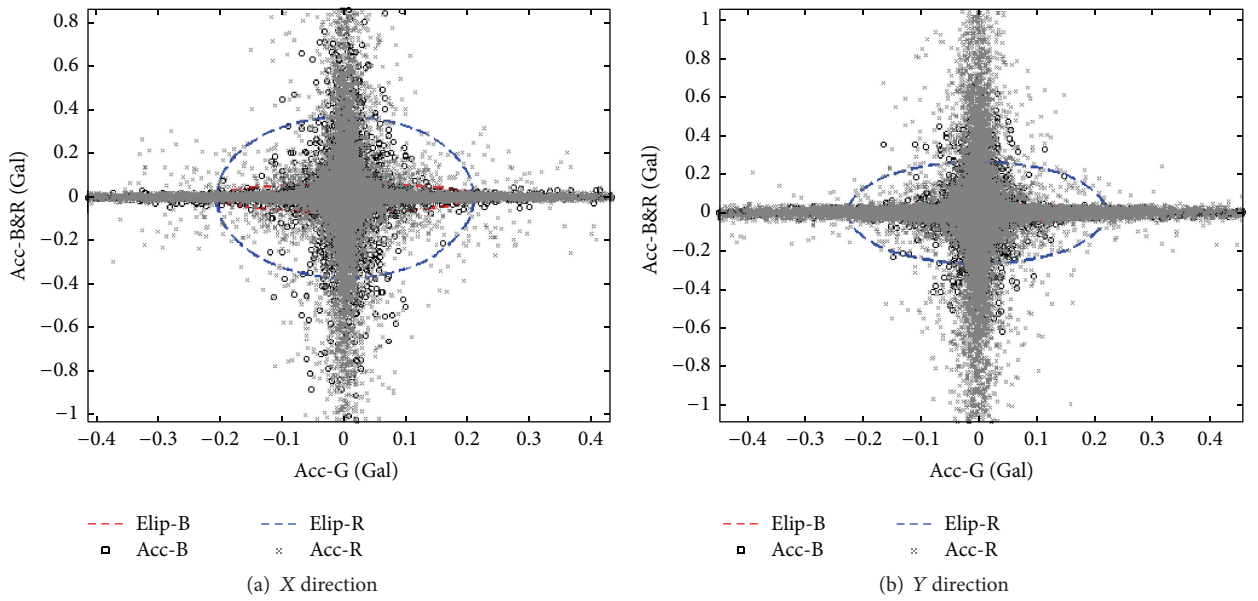

(a) X direction (b) Y direction

Figure 8: Ellipse error for the base and roof responses during the earthquake shaking.

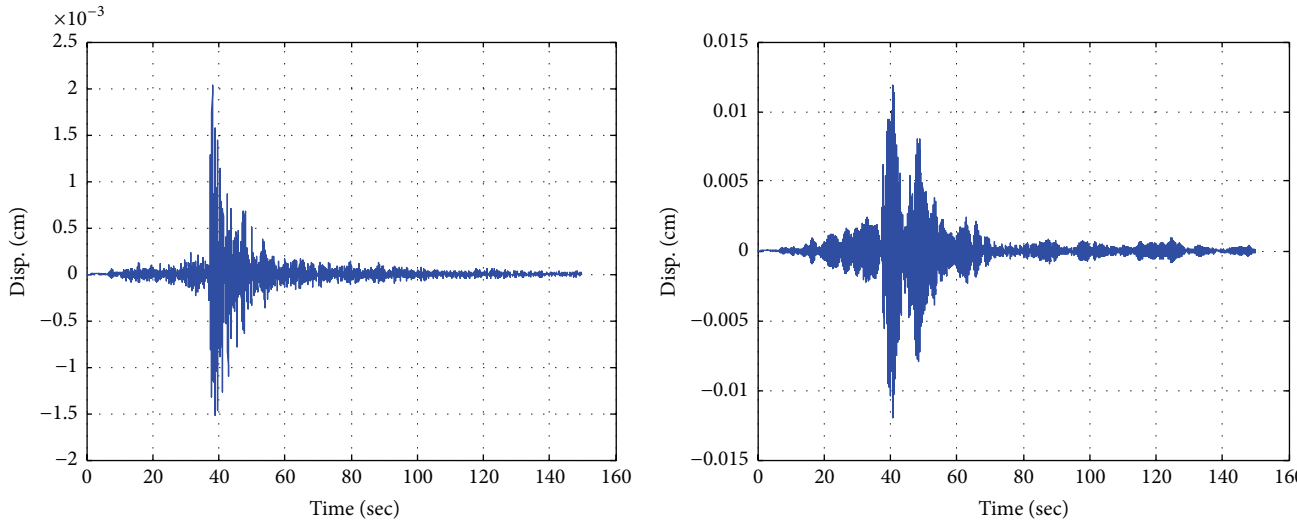

(a) Base point (b) Roof point

Figure 9: Dynamic displacement in X direction during the earthquake shaking.

3.2. Displacement and Torsion Analysis. Accelerometer sensors are used in monitoring static, semistatic, and dynamic structural performance [7]. The relations between acceleration, velocity, and displacement are governed by simple kinematics. The displacement is the integration of velocity, which in turn is the integration of acceleration. The high-pass filter is applied to the acceleration time histories, followed by double integration to extract the dynamic displacement. Sayed et al. [21] have applied 4th order Butterworth high-pass filter to efficiently extract the displacement from acceleration time history. Therefore, the 4th-order Butterworth high-pass filter is applied in this study with corner frequency 2 Hz, which exceeds the fundamental frequency of the building as will be described later.

The extracted dynamic (high frequency) displacements from the acceleration responses for the base and roof points in X direction are shown in Figure 9. The statistical values of the dynamic displacement are described in Table 4. From Figure 9 and Table 4, it can be seen that the maximum displacement occurred in roof in X direction; in addition, the standard deviation (STD) calculations illustrate that the displacements for the different recording points are within the acceptable range. In reality, all three-dimensional structures have both planned and elevation irregularity; thus, they are prepared for coupled translational and torsional responses. Moreover, there is only limited information at present on how to surpass the coupled horizontal and torsional vibration of structures, simultaneously.

Table 4: Dynamic displacement for the base and roof points (cm).

Parameters	Base point		Roof point	
	X	Y	X	Y
Max.	0.002	$7.65e-4$	0.012	0.006
Min.	−0.0015	$-8.43e-4$	−0.012	−0.006
Mean	$8.4e-10$	$5.74e-10$	$1.7e-10$	$1.32e-9$
STD	$4.3e-5$	$2.84e-5$	$4.22e-4$	$3.5e-4$

In fact, torsional response of structures subjected to dynamic earthquake or wind loading is applied for the real and experimental studies. Torsional motion is studied for the deck of long-span bridges such as Tacoma Narrows Bridges [19] and Zhujiang Huangpu Bridge [20]. Buildings are significantly vulnerable when subjected to torsional dynamic loads, especially those including asymmetric plan, which have been demonstrated from many destructive earthquake experiences. Therefore, it is important to consider this situation in the assessment of structures during earthquake shaking. However, the torsional displacement is measured to completely define the buildings movement under shaking loads. In this study, the torsional displacement of the building has been calculated with (1). Figure 10 demonstrates the diagram for the torsion displacement in X and Y directions for the building:

$$\emptyset = \arcsin\left(\frac{D}{L}\right) \times \frac{180}{\pi}, \tag{1}$$

where $\emptyset$ is a torsion angle (α) for X and (β) for Y directions as shown in Figure 10; D is the interstorey displacement for two symmetrical points in X or Y direction, as shown in Figure 10; D value equals $(X_1 - X_2)$ for elevation and $(Y_3 - Y_1)$ for plan. L is the distance between the two monitoring points, which is 33.8 m for X direction and 17.2 m for Y direction.

Figure 11 presents the torsional deformation of the roof point in the vertical plan (elevation direction or X direction) and horizontal plan (roof plan or Y direction) during the earthquake shaking. It can be seen that the significant torsional direction of building is the elevation direction with X direction. In addition, the maximum torsional deformation for the roof floor is 0.02 rad in X direction, while it is a negligible value (0.005 rad) in Y direction. The results prove that the vibration of the building in the X direction is higher and more dominant on the rotation of building in the longitudinal direction.

3.3. Wavelet and Frequency Analysis. Wavelet analysis is suitable for analyzing variations of power within signals [22]. The wavelet transform is not completely different from Fourier transform [22–24]. However, it is well-suited for analyzing signals with sharp discontinuities [23]. Windowed Fourier Transform or Short Time Fourier Transform (STFT) is more suitable for nonstationary signals. STFT basically maps a time series into a two-dimensional time series in both time and frequency domains. However, fixed frequency resolution for all frequencies is considered the main shortcoming of STFT [22–24]. The power spectrum method is considered a type

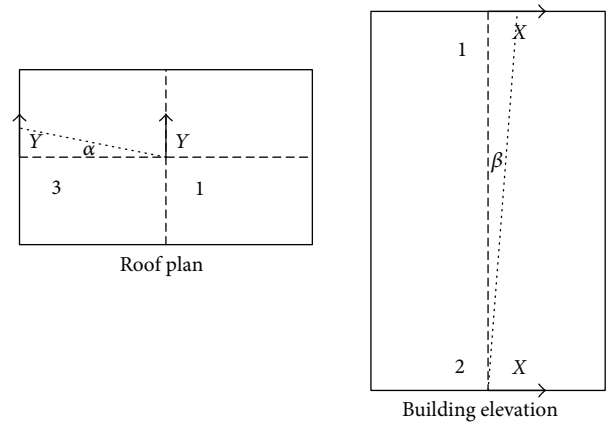

Figure 10: Torsional angle diagram view for the building.

of STFT for mapping frequencies changing in cyclist through time.

In the power spectrum, the signal is divided into segments, while the Fourier transform is calculated for these segments. The segments are multiplied by positive smooth bell-shape curves windows to avoid spectral leakage. The original signal can be reformed from the details only without any loss of information [23]. The reconstructed signal is illustrated as follows:

$$S_0(t) = \sum_{j=1}^{n} d_j(t), \tag{2}$$

where n is the total number of decomposition levels; and the detail components (d) of the original signal (S) can be expressed by the linear combination of the wavelet basis function (mother wavelet) as follows:

$$d_j(t) = \sum_{-\infty}^{\infty} C_{j,k} \psi_{j,k}, \tag{3}$$

where k represents an index of time scale, $C_{j,k}$ are the corresponding wavelet coefficients, and $\psi_{j,k}$ are the basis wavelet functions, which are expressed as

$$\psi_{j,k} = 2^{j/k} \psi\left(2^j t - k\right). \tag{4}$$

Finally, the original signal which has a time interval $[0 \quad t]$ can be expressed:

$$S_0(t) = \sum_{j=1}^{n} \sum_{k=0}^{t} C_{j,k} \psi_{j,k.} \tag{5}$$

There are many types of mother wavelets that can be defined. For discrete wavelet analysis, orthogonal wavelets (Daubechies and least-asymmetric wavelets) and B-spline biorthogonal wavelets have been commonly used [25]. In this study, the 10th-order Daubechies has been chosen. The choice to use Daubechies wavelets is motivated by their resemblance to the original signals [13]. Furthermore, the previous studies found that the Daubechies mother wavelet is

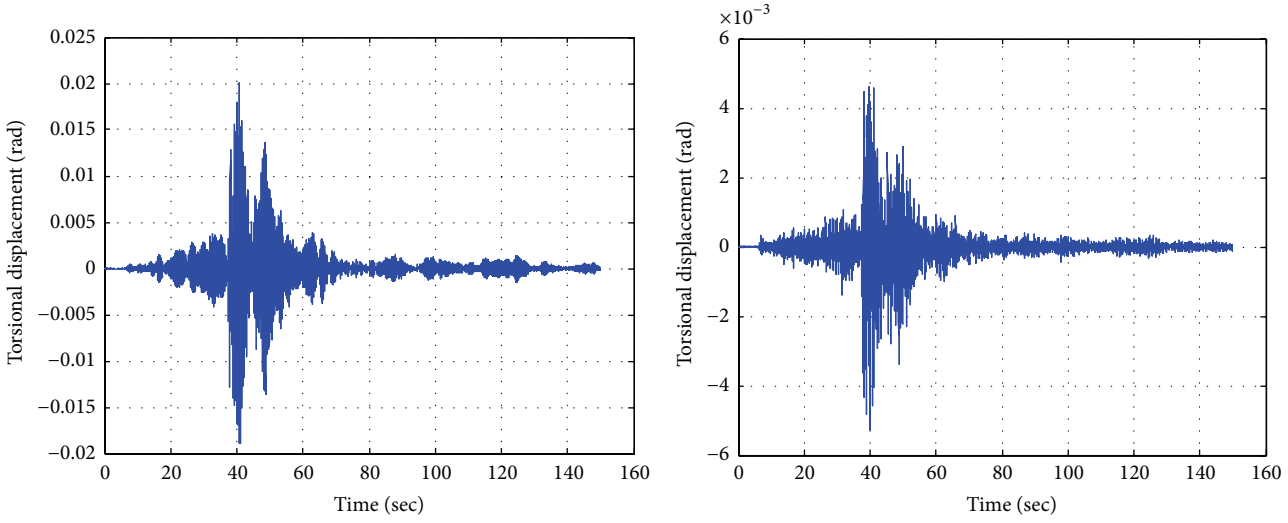

(a) X direction (b) Y direction

Figure 11: Torsional deformation of the building during shaking.

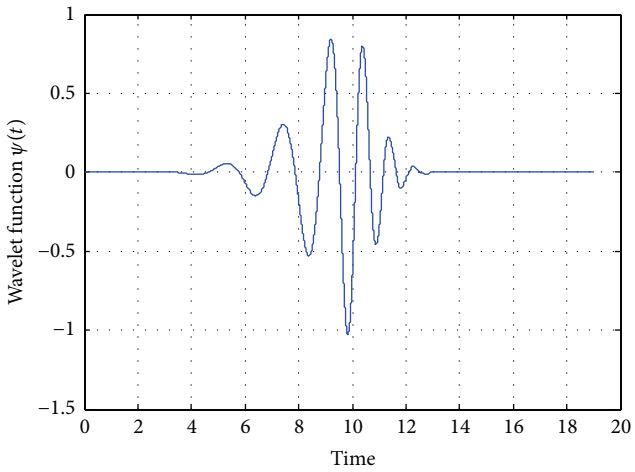

Figure 12: Daubechies basis function (db10).

suitable for the seismic performance analyses [12, 13]. Explicit form of the selected wavelet is shown in Figure 12, while the decomposition level calculations can be found in [25, 26]. In addition, the order of wavelet is used for its orthogonality and satisfactory resolution in both time and frequency domains [24, 27]. A high level of decomposition is selected in this study to present the full power performance of signal as shown in [26]. Therefore, the 9th decomposition level is selected to investigate the effectiveness of wavelet levels on the responses of the case study building due to earthquake shaking.

The recorded acceleration responses of the base and roof points in X direction are illustrated in Figure 13. From this Figure, it is shown that the peak recorded acceleration at the base point is 1.40 Gal, while it is 4.84 Gal for the roof point. In addition, the detail functions of the selected nine decomposition levels of the reconstructed details of the original recorded acceleration responses for the base and roof points during the earthquake in X direction from level 1 to level 9 are presented from top to bottom in Figure 14.

The total energy of a discrete signal is the sum of the squares of its absolute values and, therefore, the total energy of the original signal can be expressed as follows [28]:

$$E = \Delta t \sum_{t=0}^{t} S_0^2 (t) . \tag{6}$$

In addition, the total energy can be represented in the form of details only at each decomposition level:

$$E = \sum_{j=1}^{n} \sum_{t=0}^{t} d_j^2 (t) . \tag{7}$$

The energy content of the decomposition levels of the acceleration response measurements at the different monitoring points during the earthquake shaking are demonstrated in Figure 15. From this Figure, it can be noticed that the energy distribution of the acceleration responses suffer slight changes between X and Y direction for the three monitoring points. Furthermore, Figure 15(a) illustrates that level 3, which represents the frequency content (12.5–25 Hz), contains 65% of the whole energy of the acceleration response of the ground point in both directions during the earthquake shaking. Moreover, levels 3 and 4, which represent (6.25–25 Hz), contain more than 95% of the energy. Furthermore, the energy distribution of the base point in Figure 15(b) demonstrates that level 4 (6.25–12.5 Hz) contains about 50% of the acceleration response energy.

Similarly, the energy distribution of the roof point in Figure 15(c) illustrates that level 5 (3.125–6.25 Hz) contains about 60% of the whole energy of the acceleration response measurements in both directions. Therefore, during the earthquake shaking, it can be concluded that the higher the monitoring point elevation, the lower the dominant

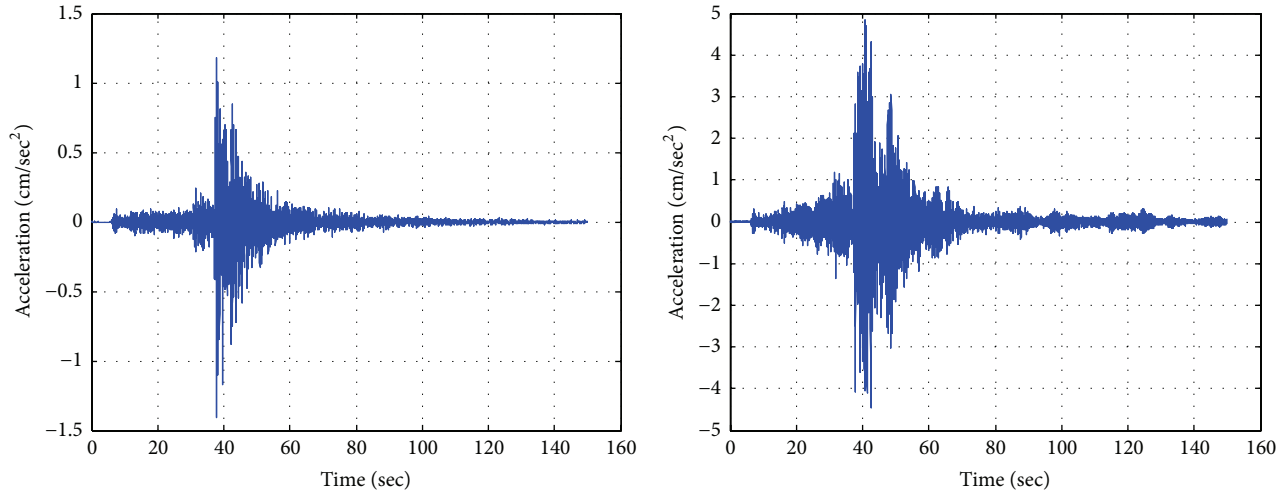

(a) Base point (b) Roof point

Figure 13: Acceleration response measurements in X direction during the earthquake shaking.

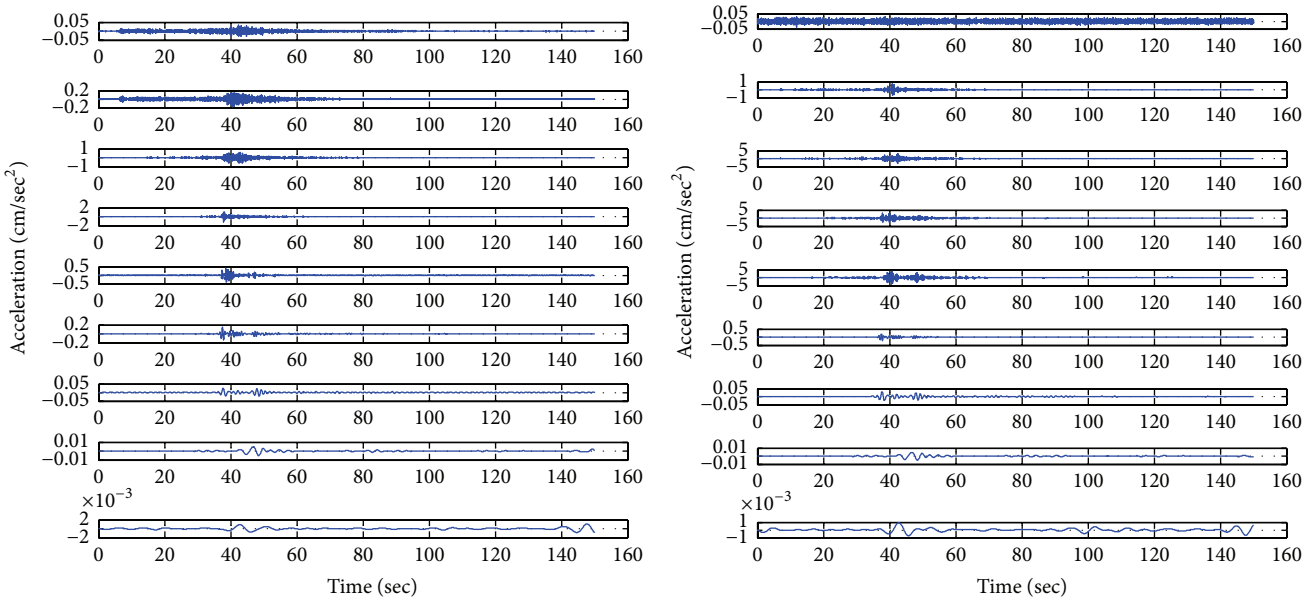

(a) Base point (b) Roof point

Figure 14: Decomposition levels of the reconstructed details for the base and roof points in X direction during earthquake shaking.

frequency range. Furthermore, the performance of various monitoring points can be compared based on the wavelet energy contents analysis.

Convenient methods such as FFT [25, 29] and wavelet spectrum [29, 30] are considered to estimate the frequency modes for the building. In wavelet spectrum analysis, scales numbers are first defined. These numbers outline the amount of stretch or compression that the wavelet achieves to map the variability of the signal in time domain at various wavelengths, where higher frequencies correspond to lower scales and vice versa. In this study, the wavelet analysis for more than 120 various scales is assumed. Consequently, the real or complex continuous components of wavelet coefficients are computed. Finally, the converts scale to pseudo-frequencies, using the sampling period of the recorded acceleration and the computed wavelet coefficients.

Figure 16 illustrates the frequency models and wavelet spectrum for the acceleration measurements at the roof point. The fundamental frequency of the measurements is 2.54 Hz. In addition, the first and fourth mode frequencies are clearly visible at the measurements in X direction; while, modes one, four, and six are visible in Y direction.

The roof vibration is more noticeable compared to the base point vibration which is based on the power spectrum density comparison between the modes of the base and roof measurements. Moreover, the wavelet spectrum results

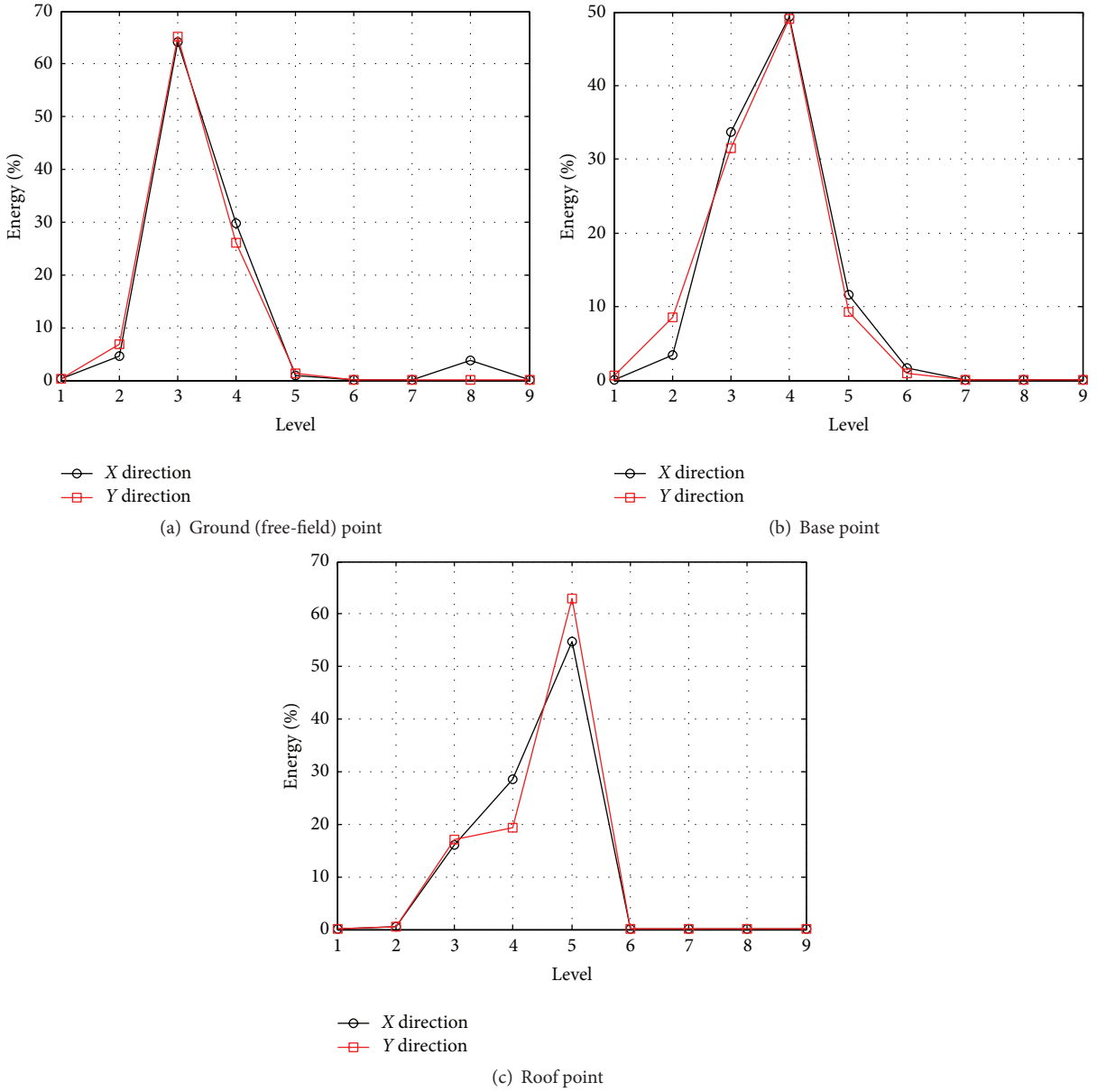

FIGURE 15: Energy distribution of the decomposition levels of the measurements points during the earthquake.

show that the dominant frequency of both base and roof points is the fundamental (first mode) frequency. This result implies the elasticity of the deformation responses of the building during the earthquake event. Finally, the wavelet and frequency methods results verify the energy contents of wavelet analysis to be an efficient tool in investigating the effect of earthquake events on the frequency content of structural responses and hence it is a powerful tool in structural performance assessment.

4. Conclusions

This study proposes a low cost acceleration SHM system to assess the structural performance of the administration building in Seoul National University of Education, South Korea. The statistical (ellipse errors and covariance and linear fitting analyses) and wavelet analysis (power content and frequency analyses) methods are applied to investigate and assess the performance of the building during an earthquake shaking. The conclusions drawn from this study are as follows.

The statistical analysis results illustrated that the roof acceleration responses are higher than for the base point. Moreover, the roof torsional deformations are increased by 50% during the earthquake shaking in the two directions, while the base torsional deformations are small during the earthquake shaking. The rotation occurred for the base point, while the hyperbolic rotation occurred for the roof point in

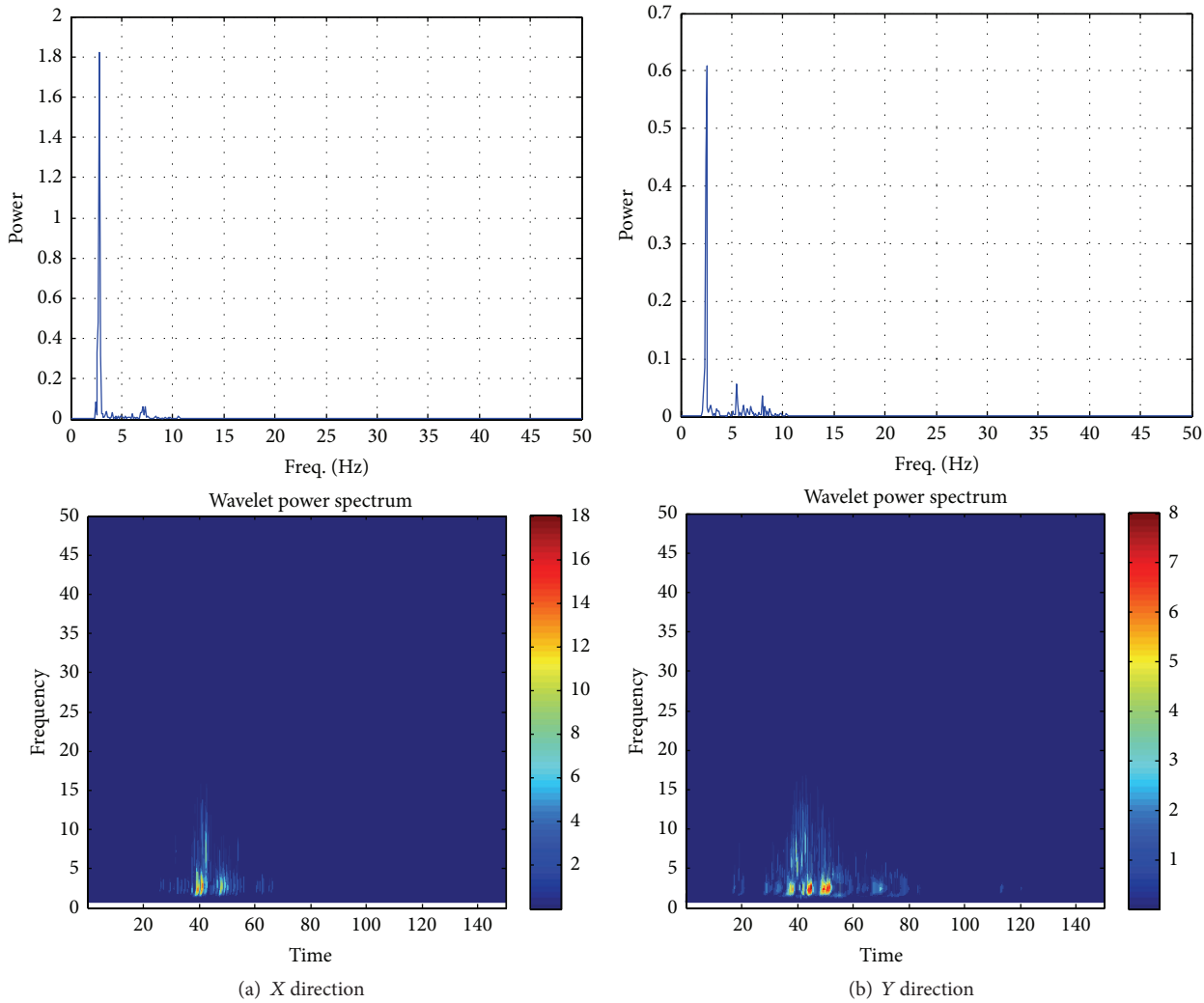

(a) X direction (b) Y direction

Figure 16: Frequency models and wavelet spectrum of roof point for X and Y direction.

the two directions. In addition, the roof eigenvalues and eigenvector are greater than for the base in the two directions, which assure the higher responses for the roof under the earthquake shaking. Finally, the statistical calculations and analysis illustrated that the displacements of the different recording points are within the acceptable range, which indicate building safety during the earthquake event.

The wavelet analysis results showed that the monitoring points frequency contents suffer slight changes between X and Y directions. In addition, it can be seen that the dominant frequency ranges are shown as 12.5–25 Hz, 6.25–25 Hz, and 3.125–6.25 Hz in both directions for ground, base, and roof points, respectively. Furthermore, it can be observed that the dominant frequency range (6.25–25 Hz) contains more than 95% of the energy. In addition, it can be concluded that the higher the monitoring point elevation, the lower the dominant frequency range that occurred during the earthquake shaking. Therefore, during earthquake shaking, it is understood that higher the elevation reveals lower dominant frequency range.

The roof vibration is more noticeable compared to the base point vibration which is based on the power spectrum density comparison between the modes of the base and roof measurements. Moreover, the wavelet spectrum results show that the dominant frequency of both base and roof points is the fundamental (first mode) frequency. This result implies the elasticity of the deformation responses of the building during the earthquake event. Furthermore, the wavelet and frequency methods results verify the energy contents of wavelet analysis to be an efficient tool in investigating the effect of earthquake events on the frequency content of structural responses and hence it is a powerful tool in structural performance assessment.

Finally, the aforementioned results indicated that the proposed low cost acceleration monitoring system

which consists of three acceleration sensors, dataloggers, and a storage PC has proven its efficiency in investigating and assessing the structural performance of the building during the earthquake shaking.

Conflict of Interests

The authors declare that there is no conflict of interests regarding the publication of this paper.

Acknowledgment

This research was supported by a grant (14CTAP-C078944-01) from Technology Advancement Research Program funded by Ministry of Land, Infrastructure and Transport of Korean government.

References

[1] M. Gul and F. N. Catbas, "Statistical pattern recognition for Structural Health Monitoring using time series modeling: theory and experimental verifications," *Mechanical Systems and Signal Processing*, vol. 23, no. 7, pp. 2192–2204, 2009.

[2] M. Çelebi, "Seismic monitoring of structures and new developments," in *Earthquakes and Health Monitoring of Civil Structures*, Springer Environmental Science and Engineering, chapter 2, pp. 37–84, Springer, Dordrecht, The Netherlands, 2013.

[3] F. P. Kopsaftopoulos and S. D. Fassois, "Vibration based health monitoring for a lightweight truss structure: experimental assessment of several statistical time series methods," *Mechanical Systems and Signal Processing*, vol. 24, no. 7, pp. 1977–1997, 2010.

[4] C. W. Follen, M. Sanayei, B. R. Brenner, and R. M. Vogel, "Statistical bridge signatures," *Journal of Bridge Engineering*, vol. 19, no. 7, Article ID 04014022, 2014.

[5] S. D. Fassois and J. S. Sakellariou, "Time-series methods for fault detection and identification in vibrating structures," *Philosophical Transactions of the Royal Society A: Mathematical, Physical and Engineering Sciences*, vol. 365, no. 1851, pp. 411–448, 2007.

[6] Y.-L. Ding, G.-X. Wang, P. Sun, L.-Y. Wu, and Q. Yue, "Long-term structural health monitoring system for a high-speed railway bridge structure," *The Scientific World Journal*, vol. 2015, Article ID 250562, 17 pages, 2015.

[7] M. R. Kaloop, M. A. Sayed, D. Kim, and E. Kim, "Movement identification model of port container crane based on structural health monitoring system," *Structural Engineering and Mechanics*, vol. 50, no. 1, pp. 105–119, 2014.

[8] M. R. Kaloop and J. W. Hu, "Stayed-cable bridge damage detection and localization based on accelerometer health monitoring measurements," *Shock and Vibration*, vol. 2015, Article ID 102680, 11 pages, 2015.

[9] V.-N. Dinh, B. Basu, and R. B. J. Brinkgreve, "Wavelet-based evolutionary response of multispan structures including wave-passage and site-response effects," *Journal of Engineering Mechanics*, vol. 140, no. 8, Article ID 04014056, 2014.

[10] V. Kumar, S. K. Gawre, and T. Kumar, "Power quality analysis using wavelet transform: a review," *International Journal of Innovative Research in Science, Engineering and Technology*, vol. 3, no. 3, pp. 130–136, 2014.

[11] D.-A. Tibaduiza, M.-A. Torres-Arredondo, L. E. Mujica, J. Rodellar, and C.-P. Fritzen, "A study of two unsupervised data driven statistical methodologies for detecting and classifying damages in structural health monitoring," *Mechanical Systems and Signal Processing*, vol. 41, no. 1-2, pp. 467–484, 2013.

[12] S. B. Ali and D. Kim, "Wavelet analysis of the seismic response of a base-isolated nuclear power plant structure considering soil-structure interaction," SMiRT-23 Division V, Paper 270, Manchester, UK, 2015.

[13] F. Mollaioli and A. Bosi, "Wavelet analysis for the characterization of forward-directivity pulse-like ground motions on energy basis," *Meccanica*, vol. 47, no. 1, pp. 203–219, 2012.

[14] V. Besharat, M. Davoodi, and M. K. Jafari, "Variations in ground surface responses under different seismic input motions due the presence of a tunnel," *Arabian Journal for Science and Engineering*, vol. 39, no. 10, pp. 6927–6941, 2014.

[15] H. Li, T. Yi, M. Gu, and L. Huo, "Evaluation of earthquake-induced structural damages by wavelet transform," *Progress in Natural Science*, vol. 19, no. 4, pp. 461–470, 2009.

[16] M. B. Nigro, S. N. Pakzad, and S. Dorvash, "Localized structural damage detection: a change point analysis," *Computer-Aided Civil and Infrastructure Engineering*, vol. 29, no. 6, pp. 416–432, 2014.

[17] R. Yao and S. N. Pakzad, "Autoregressive statistical pattern recognition algorithms for damage detection in civil structures," *Mechanical Systems and Signal Processing*, vol. 31, pp. 355–368, 2012.

[18] S. Arangio and F. Bontempi, "Structural health monitoring of a cable-stayed bridge with Bayesian neural networks," *Structure and Infrastructure Engineering*, vol. 11, no. 4, pp. 575–587, 2015.

[19] H. S. Park, H. G. Sohn, I. S. Kim, and J. H. Park, "Application of GPS to monitoring of wind-induced responses of high-rise buildings," *Structural Design of Tall and Special Buildings*, vol. 17, no. 1, pp. 117–132, 2008.

[20] M. R. Kaloop, "Bridge safety monitoring based-GPS technique: case study Zhujiang Huangpu Bridge," *Smart Structures and Systems*, vol. 9, no. 6, pp. 473–487, 2012.

[21] M. A. Sayed, S. Go, S. G. Cho, and D. Kim, "Seismic responses of base-isolated nuclear power plant structures considering spatially varying ground motions," *Structural Engineering and Mechanics*, vol. 54, no. 1, pp. 169–188, 2015.

[22] C. Torrence and G. P. Compo, "A practical guide to wavelet analysis," *Bulletin of the American Meteorological Society*, vol. 79, no. 1, pp. 61–78, 1998.

[23] R. Z. Sarica and M. S. Rahman, "A wavelet analysis of ground motion characteristics," in *Proceedings of the U.S.-Taiwan Workshop on Soil Liquefaction, Taiwan*, 2003.

[24] C. Sunde, *Wavelet and spectral analysis of some selected problems in reactor diagnostics [Licentiate Degree Thesis]*, Department of Reactor Physics, Chalmers University of Technology, Gothenburg, Sweden, 2004.

[25] Y. Seo, S. Kim, O. Kisi, and V. P. Singh, "Daily water level forecasting using wavelet decomposition and artificial intelligence techniques," *Journal of Hydrology*, vol. 520, pp. 224–243, 2015.

[26] Y.-F. Sang, D. Wang, and J.-C. Wu, "Entropy-based method of choosing the decomposition level in wavelet threshold denoising," *Entropy*, vol. 12, no. 6, pp. 1499–1513, 2010.

[27] J. Iyama and H. Kuwamura, "Application of wavelets to analysis and simulation of earthquake motions," *Earthquake Engineering and Structural Dynamics*, vol. 28, no. 2-3, pp. 255–272, 1999.

[28] J. S. Walker, *A Primer on Wavelets and Their Scientific Applications*, Chapman & Hall/CRC, New York, NY, USA, 2nd edition, 1999.

[29] MathWorks, *MATLAB, The Language of Technical Computing*, MathWorks, Natick, Mass, USA, 2009.

[30] M. H. Trauth, *MATLAB Recipes for Earth Sciences*, Springer, 3rd edition, 2010.